

ORIGINAL ARTICLE

MiR-520h-mediated FOXC2 regulation is critical for inhibition of lung cancer progression by resveratrol

Y-H Yu^{1,2,16}, H-A Chen^{3,4,16}, P-S Chen^{5,6}, Y-J Cheng⁷, W-H Hsu¹, Y-W Chang⁸, Y-H Chen⁹, Y Jan¹⁰, M Hsiao¹⁰, T-Y Chang⁷, Y-H Liu⁹, Y-M Jeng¹¹, C-H Wu^{3,4}, M-T Huang^{3,4}, Y-H Su^{3,4}, M-C Hung^{7,9}, M-H Chien^{3,12}, C-Y Chen¹³, M-L Kuo^{5,6} and J-L Su^{7,9,14,15}

Resveratrol, a phytochemical found in various plants and Chinese herbs, is associated with multiple tumor-suppressing activities, has been tested in clinical trials. However, the molecular mechanisms involved in resveratrol-mediated tumor suppressing activities are not yet completely defined. Here, we showed that treatment with resveratrol inhibited cell mobility through induction of the mesenchymal–epithelial transition (MET) in lung cancer cells. We also found that downregulation of FOXC2 (forkhead box C2) is critical for resveratrol-mediated suppression of tumor metastasis in an *in vitro* and *in vivo* models. We also identified a signal cascade, namely, resveratrol–miRNA-520h–PP2A/C–Akt→NF-κB→FOXC2, in which resveratrol inhibited the expression of FOXC2 through regulation of miRNA-520h-mediated signal cascade. This study identified a new miRNA-520h-related signal cascade involved in resveratrol-mediated tumor suppression activity and provide the clinical significances of miR-520h, PP2A/C and FOXC2 in lung cancer patients. Our results indicated a functional link between resveratrol-mediated miRNA-520h regulation and tumor suppressing ability, and provide a new insight into the role of resveratrol-induced molecular and epigenetic regulations in tumor suppression.

Oncogene advance online publication, 12 March 2012; doi:10.1038/onc.2012.74

Keywords: FOXC2; miR-520h; resveratrol; metastasis

INTRODUCTION

Metastasis, a multistep process involving the dissemination of cancer cells from primary tumors to establish secondary tumors in distant organs and act as a common cause of death in cancer patients.¹ Recently, the concept of the epithelial–mesenchymal transition (EMT), as developed in the field of embryology, has been extended to cancer progression and metastasis.² The biological significance of EMT has been proven in animal models and clarified in tumor samples by EMT-associated markers, such as the mesenchymal markers of Fibronectin, N-cadherin,³ and Vimentin,⁴ and the epithelial marker of E-cadherin.⁵ Epithelial cells undergoing EMT must generate functional and morphological changes. Multiple complex signaling systems are required to induce EMT, such as the TGF-β, Wnt signaling and notch pathways.^{6–7} Some transcriptional factors, such as the zinc-finger proteins Snail⁸ and Slug,⁹ the E-box-binding protein ZEB1,¹⁰ the basic helix-loop-helix protein Twist,¹¹ the homeobox protein Gooseoid¹² and the forkhead box protein FOXC2,¹³ are involved in regulating EMT-related factors.

Overexpression of FOXC2 has been shown to activate EMT and to correlate with tumor metastasis.¹⁴ Recent report suggests that FOXC2 could be an important prognostic indicator for esophageal cancer patients as it is involved in cancer progression and associated with poor prognosis.¹⁵ An *in vivo* study found that

FOXC2 enhanced the ability of mouse mammary carcinoma cells metastasize to the lungs, and FOXC2 expression is significantly correlated with a highly aggressive basal-like subtype of human breast cancers.¹³ These observations indicate the central role of FOXC2 in promoting invasion and metastasis and suggest that it may be a potential biomarker for cancer progression.

Resveratrol (*trans*-3, 5, 4'-trihydroxystilbene) is a polyphenol that has been found in various plants and Chinese herbs.¹⁶ It inhibits cancer progression at the initiation, promotion and progression steps, and it also has chemoprevention abilities through inhibiting molecular target such as kinases, cyclooxygenases, ribonucleotide reductase and DNA polymerases.¹⁷ Resveratrol inhibits several transcriptional factors associated with EMT and the key guardians of cell survival, NF-κB¹⁸ and AP-2,¹⁹ and downregulates protein kinases such as IκB kinase,¹⁸ AMPK,²⁰ JNK, MAPK, ERK1/2,²¹ Akt,²² PKC²³ and PKD.²⁴

Seeking and investigating compounds with medicinal effects from natural products has become a new trend, as evidenced by the successful use of two representative drugs, paclitaxol, extracted from *Taxus brevifolia* and vinorelbine, derived from the periwinkle plant, to treat several clinical cancers. Resveratrol is presently in phase I clinical trials for human colon and colorectal cancers.¹⁶ However, the molecular mechanisms involved in resveratrol-mediated tumor-suppressing activities are not yet

¹Department of Internal Medicine, Divisions of Pulmonary and Critical Care Medicine, China Medical University Hospital, Taichung, Taiwan; ²Graduate Institute of Clinical Medical Science, China Medical University, Taichung, Taiwan; ³Graduate Institute of Clinical Medicine, College of Medicine, Taipei Medical University, Taipei, Taiwan; ⁴Department of Surgery, Division of General Surgery, Shuang Ho Hospital, Taipei Medical University, Taipei, Taiwan; ⁵Institute of Toxicology, College of Medicine and Angiogenesis Research Center, National Taiwan University, Taipei, Taiwan; ⁶Department of Oncology, National Taiwan University Hospital, Taipei, Taiwan; ⁷Graduate Institute of Cancer Biology, College of Medicine, China Medical University, Taichung, Taiwan; ⁸Graduate Institute of Biochemistry and Molecular Biology, National Yang-Ming University, Taipei, Taiwan; ⁹Center for Molecular Medicine, China Medical University Hospital, Taichung, Taiwan; ¹⁰The Genomics Research Center, Academia Sinica, Taipei, Taiwan; ¹¹Department of Pathology, National Taiwan University Hospital, Taipei, Taiwan; ¹²Wan Fang Hospital, Taipei Medical University, Taipei, Taiwan; ¹³Cancer Center, China Medical University Hospital, Taichung, Taiwan; ¹⁴Cancer Biology and Drug Discovery Ph.D. Degree Program, China Medical University, Taichung, Taiwan and ¹⁵Department of Biotechnology, Asia University, Taichung, Taiwan. ¹⁶These authors contributed equally to this work. Correspondence: Professor J-L Su, Graduate Institute of Cancer Biology, College of Medicine, China Medical University, No.91, Hsueh-Shih Road, Taichung 40402, Taiwan. E-mail: jlsu@mail.cmu.edu.tw or M-H Chien, Graduate Institute of Clinical Medicine, College of Medicine, Taipei Medical University, Taipei, Taiwan. E-mail: mhchien1976@gmail.com

Received 13 August 2011; revised 2 January 2012; accepted 31 January 2012

completely defined. It is critical and timely to understand the detailed molecular mechanisms that associate with resveratrol-mediated antitumor activity in order to develop future resveratrol-related clinical trials. Thus, we examined the signaling pathway involved in resveratrol-mediated tumor suppression in lung cancer cells.

This study identified a signal cascade, resveratrol –| miRNA-520h –| PP2A/C –| Akt → NF-κB → FOXC2, in which resveratrol inhibited the expression of FOXC2 by downregulating miRNA-520h and the signal cascade. Our results indicated a functional link between resveratrol-mediated miRNA-520h regulation and tumor suppressing ability, and provide a new insight into the role of resveratrol-induced molecular and epigenetic regulations in tumor suppression.

RESULTS

Downregulation of FOXC2 is critical for resveratrol-mediated tumor suppression

The EMT and the reversed process, mesenchymal–epithelial transition (MET), have been shown to have an important role in regulating invasion and migration of cancer cells. The ability of resveratrol to inhibit the cell mobility of lung cancer cells was elucidated by treating CL1-5 and A549 non-small cell lung cancer cells with various concentrations of resveratrol. Treatment with resveratrol decreased the ability of lung cancer cells to migrate and invade in a dose-dependent manner (Figure 1a). The ability of resveratrol to inhibit cell mobility was confirmed by time-lapse microscopy that traced cell mobility after resveratrol treatment (Supplementary Figure S1A).

The EMT involves losing epithelial differentiation and acquiring a mesenchymal phenotype that allows cancer cells to detach from the primary tumor mass. Disseminated cancer cells lose expression of the epithelial marker E-cadherin that regulates cell-to-cell contact and they acquire such mesenchymal markers such as Fibronectin, N-cadherin and Vimentin. The effects of resveratrol in the MET of lung cancer cells were examined by treating CL1-5 cells with resveratrol for 48 h and observing cell morphology by phase-contrast microscopy. Resveratrol-treated CL1-5 cells had cell morphology that changed from spindle-shaped to epithelial characteristics (Supplementary Figure S1B). Treatment with resveratrol increased the expression of E-cadherin and decreased the expression of the mesenchymal markers of Fibronectin, N-cadherin and Vimentin in various lung cancer cell lines (Figure 1b). These data indicated that decreased cell mobility after resveratrol treatment may be due to the induction of the MET.

The molecular mechanisms involved in resveratrol-induced MET were elucidated by investigating the expression of several EMT-related transcriptional factors. Treatment with resveratrol significantly decreased the expression of FOXC2 in CL1-5 and A549 cells, but had less or undetectable effects on other transcriptional factors, such as Twist, Slug, Snail, ZEB1 and Goosecoid (Figure 1c). Resveratrol had an inhibitory effect on FOXC2 expression in the protein and mRNA levels of several lung cancer cell lines (Figure 1d). In addition, treatment with resveratrol decreased FOXC2 expression in a dose-dependent manner (Supplementary Figure S1C). These data suggest that downregulating FOXC2 is important for the resveratrol-induced MET.

The FOXC2 expressing vector was ectopically expressed in A549 and H460 lung cancer cells to investigate whether FOXC2 is involved in resveratrol-mediated repression of cell mobility in lung cancer cells. Overexpressing FOXC2 in A549 (A549/FOXC2) and H460 (H460/FOXC2) decreased E-cadherin expression and increased the expression of the mesenchymal markers N-cadherin and Vimentin (Figure 1e and Supplementary Figure S1D). It was therefore of interest to determine whether resveratrol-induced MET were exerted through the regulation of FOXC2. Stably expressing FOXC2 in A549 cells found increased ability of the cells to migrate and invade. Stably expressing FOXC2 rescued the

resveratrol-mediated suppression of cell mobility (Figure 1f) and the expression of EMT markers (Figure 1e). These results indicated that resveratrol-mediated the induction of the MET by down-regulating FOXC2 expression in lung cancer cells.

The possibility that resveratrol decreases the aggravation of lung cancer was explored by investigating the effects of resveratrol on tumor growth in an animal model. A luciferase-labeled control vector expressed A549 cells (A549/VC) and A549/FOXC2 cells were subcutaneously injected into severe combined immunodeficient mice. The A549/FOXC2-bearing mice showed slightly increased tumor volume and rescued resveratrol-mediated tumor suppression compared with A549/VC mice (Figure 2a). We further investigated the role of FOXC2 in resveratrol-mediated antimetastatic lung colony formation by detecting metastatic lung colonization in experimental metastasis models using the bioluminescence system. Tail-vein injections transplanted A549/VC cells or A549/FOXC2 cells into severe combined immunodeficient mice, which were then treated either with or without resveratrol. The A549/VC mice treated with resveratrol had inhibited lung colonization (Figure 2b, right panel, lane 1 versus lane 2). The A549/FOXC2 mice had increased lung colony formation as revealed by bioluminescence imaging analysis (Figure 2b, right panel, lane 1 versus lane 3) that was not inhibited by resveratrol treatment (Figure 2b, right panel, lane 3 versus lane 4). The metastatic nodules in the lungs were dissected from each mouse and quantified by dissecting microscopy. The number of lung metastases was reduced in A549/VC mice treated with resveratrol, but not in the A549/FOXC2-bearing mice (Figure 2c). These observations suggest the involvement of FOXC2 in *in vitro* migration/invasion, *in vivo* tumorigenesis and lung colonization activity of lung cancer cells. These data also suggest that resveratrol, through suppressing FOXC2, may act as a therapeutic agent for cancer treatment.

The prognostic significance of FOXC2 expression was determined with 96 human lung cancer specimens that had clinical follow-up records. Representative examples with different FOXC2 scores are shown in Supplementary Figure S2A. The relationships between the levels of FOXC2 expression and the clinicopathological characteristics of lung cancer are summarized in Table 1. Among these specimens, high-FOXC2 expression levels (scores of 2 and 3) strongly correlated with reduced overall survival (Figure 2d) and disease-free interval (Figure 2e) compared with tumors with low-FOXC2 expression levels (scores of 0 and 1). Our data indicate that higher levels of FOXC2 predict poor prognosis in lung cancer.

NF-κB is involved in resveratrol-mediated FOXC2 regulation

The regulatory mechanism of resveratrol participating in the transcriptional regulation of FOXC2 gene was explored through FOXC2 promoter–reporter deletion constructs (F1–F6) (Figure 3a). Resveratrol significantly decreased luciferase activity in cells transfected with the F1 and F3–F6 promoter–reporter deletion constructs, but not with F2 deletion construct (Figure 3a). The shortest construct to respond to resveratrol treatment was F6, which we analyzed for resveratrol-regulated response elements by the TESS 2.0/TFSEARCH ver1.3 software²⁵ and find four candidate response elements: NF-κB, MZF-1, AP-2α and E2F. We ascertained which of these response elements participated in regulating FOXC2 promoter activity in response to resveratrol through the use of FOXC2 promoter–reporter (F6) mutation constructs with these mutated transcription factor-binding elements (Figure 3b). Compared with wild type, resveratrol decreased promoter activity by 50–60% in the F6, F6/mutMZF-1, F6/mutAP-2α and F6/mutE2F reporters, but not in the F6/mutNF-κB reporter (Figure 3c). These results from the luciferase reporter assay indicated that NF-κB-binding element is critical for resveratrol-mediated suppression of FOXC2 promoter activity. The nuclear transcription factor NF-κB

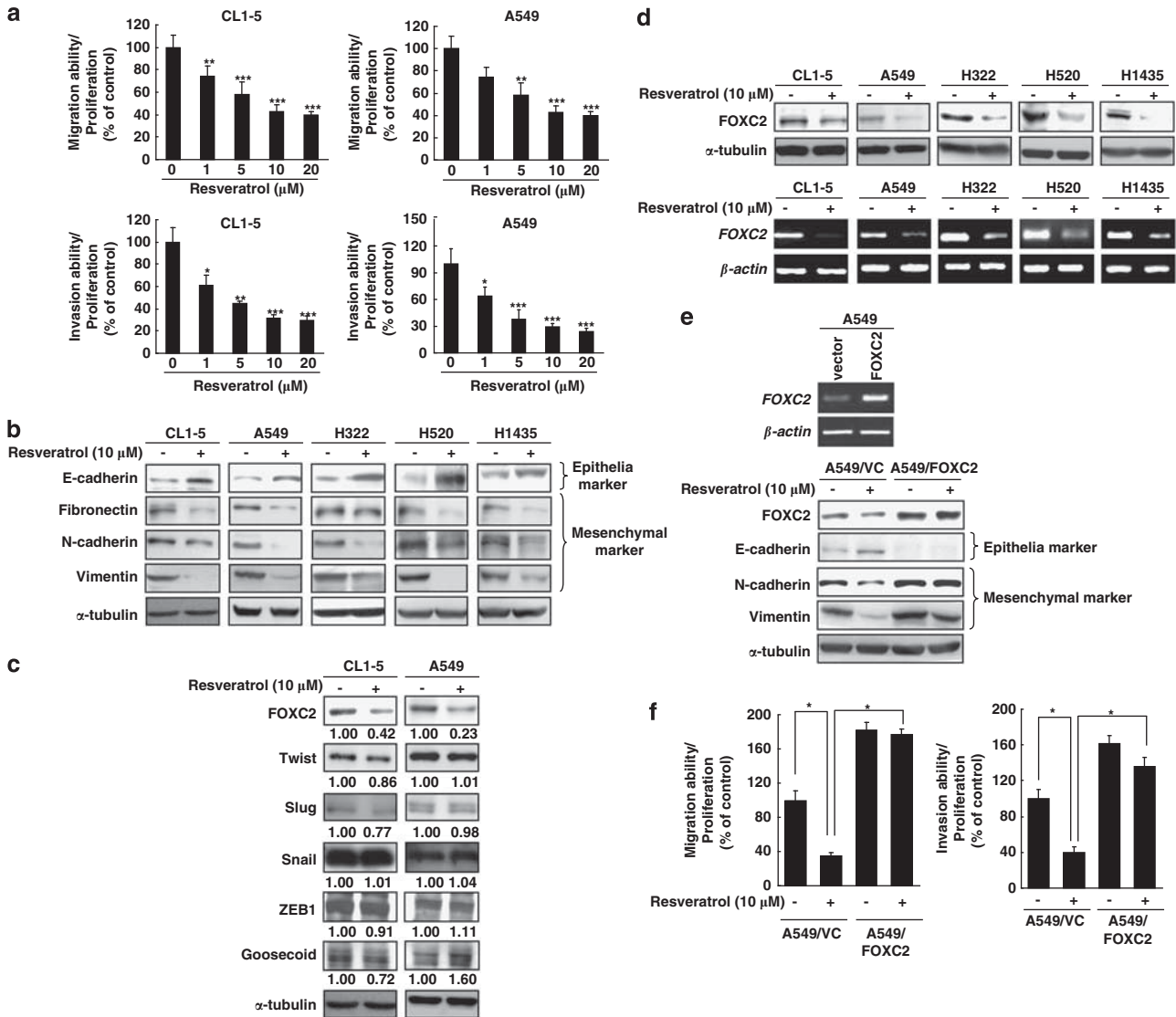


Figure 1. Resveratrol inhibits cell mobility and induces MET through regulation of FOXC2 in lung cancer cells. **(a)** CL1-5 and A549 cells were treated by the indicated concentrations of resveratrol for the transwell migration and Matrigel invasion assays. Data are representative of at least three independent experiments performed in triplicate. Asterisks denote a significant difference compared with the values for the untreated control (*indicates $P < 0.05$; **, $P < 0.01$ and ***, $P < 0.001$). **(b)** EMT markers were expressed in resveratrol-treated lung cancer cells. Lysates were collected from cells cultured with or without 10 μM resveratrol for 48 h. All experiments were performed in at least three separate experiments. **(c)** The expression levels of EMT-related transcriptional factors in resveratrol-treated lung cancer cells were measured from lysates collected from CL1-5 and A549 cells cultured with or without 10 μM resveratrol, with changes in quantities values shown with the indicated bands. **(d)** The effects of resveratrol on FOXC2 expression in lung cancer cells were analyzed by immunoblot (top) and RT-PCR (bottom) of samples from resveratrol-treated lung cancer cell lines. **(e)** Analyzed the regulation of EMT markers by FOXC2 in resveratrol-treated cells. FOXC2 expression was analyzed by RT-PCR in A549 cells overexpressing control vector or FOXC2 (upper panel). The expression of EMT markers was analyzed in the absence or presence of resveratrol in A549/VC cells and A549/FOXC2 cells (lower panel). **(f)** The indicated concentrations of resveratrol were added to the cells to measure the function of FOXC2 in resveratrol-suppressed migration and invasion. Bars represent means \pm s.d., and asterisks denote a significant difference (* indicates $P < 0.05$). Data are representative of at least three independent experiments performed in triplicate.

could promote tumorigenesis and has been linked to cellular transformation, proliferation, angiogenesis and metastasis.²⁶ We verified the ability of resveratrol to decrease the association of NF-κB with the FOXC2 promoter by a chromatin immunoprecipitation assay. The NF-κB component p65 had decreased ability to bind to the NF-κB response element on the FOXC2 promoter after resveratrol treatment (Figure 3d). As NF-κB is important for resveratrol-mediated regulation of FOXC2 promoter, the effects of resveratrol on p65 expression and nuclear translocation were

explored by immunoblot (Figure 3e) and immunofluorescence staining (Supplementary Figure S2B), which found decreased p65 protein expression in the nucleus after resveratrol treatment (Figure 3e). Genetically knocking down NF-κB subunit, p65, by expressing specific p65 siRNA (sip65) and treatment with specific NF-κB activation inhibitor IV suppressed NF-κB activity in the F6 reporter, but not in the F6/mutNF-κB reporter (Figure 3f). Furthermore, treatment with sip65 or NF-κB activation inhibitor IV also decreased the cell migration and invasion ability (Figure 3g).

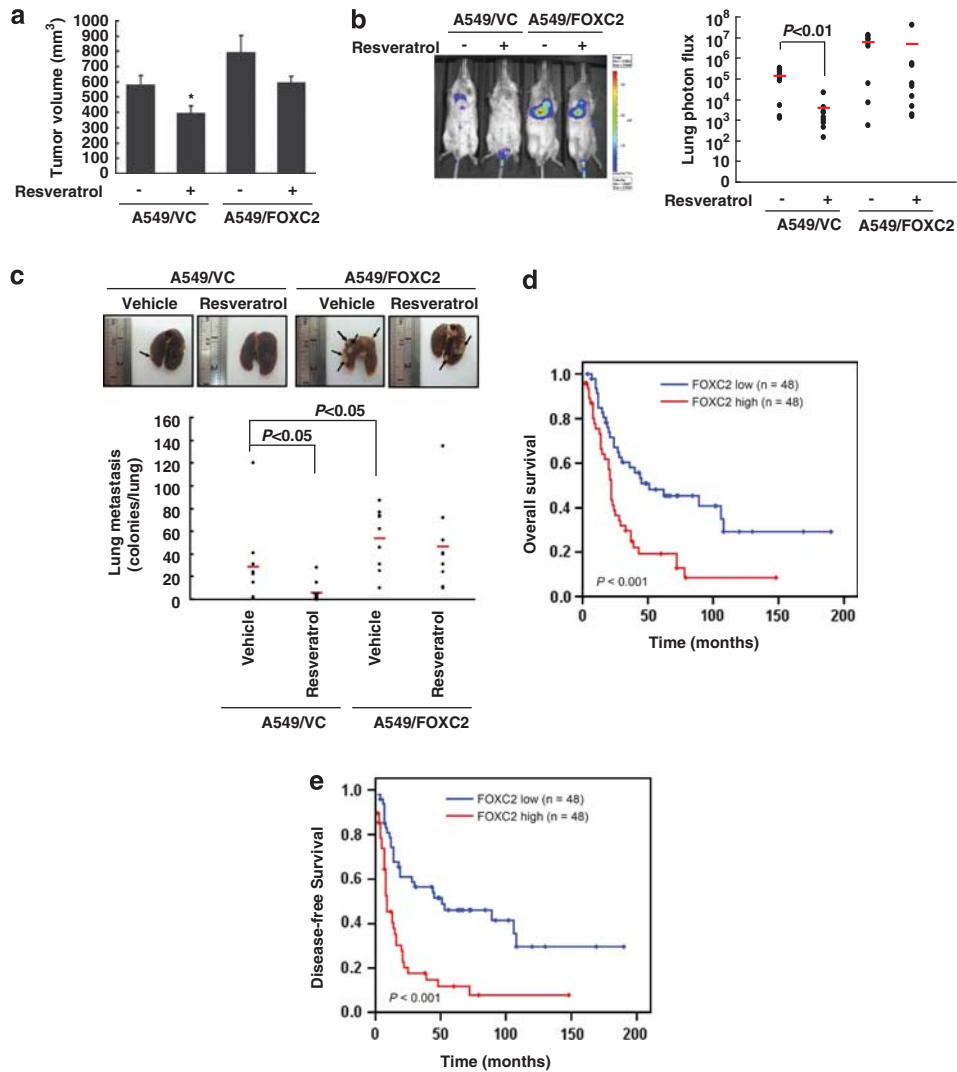


Figure 2. Biological significance of FOXC2 in cancer progression in animal model and lung cancer patients. **(a)** FOXC2 affected resveratrol-suppressed tumor growth in xenograft severe combined immunodeficient (SCID) mice (10 mice for each group) that had A549/VC and A549/FOXC2 cells subcutaneously injected and tumor volumes determined 6 weeks later. **(b)** The A549/VC and A549/FOXC2 cells stably expressing luciferase were injected into SCID mice by tail vein injection, and lung colonizations were bioluminescently imaged after 8 weeks (left) with the mean signal for each group ($n = 9$) indicated (right). **(c)** The mice (10 mice for each group) were killed 3 months after the injections and total numbers of metastatic colonies (arrows) in the lungs were counted and photographed. **(d, e)** The FOXC2 level, as determined by IHC staining, predicted a poor clinical outcome in 96 lung cancer patients when a two-sided log-rank test compared differences between groups. The Kaplan–Meier curves illustrate analyses of overall **(d)** and disease-free **(e)** survival in lung cancer patients.

PP2A/C-induced Akt inactivation is required for resveratrol-mediated suppression of NF- κ B activity, FOXC2 expression and cell mobility

Activation of phosphatidylinositol 3-kinase/Akt and ERK1/2 signaling pathways has been reported to have an important role for FOXC2 expression in adipocytes²⁷ and endothelial cells,²⁸ but the molecular mechanisms involved in expressing FOXC2 that lead to subsequent cell mobility and in regulating EMT in lung cancer cells are not clear. To define the signaling pathway involved in FOXC2 regulation by resveratrol, A549 cells were treated with the phosphatidylinositol 3-kinase/Akt inhibitor, LY294002, and with the MEK inhibitor, U0126. The expression of FOXC2 was analyzed by immunoblots (Figure 4a) and reporter activity assays (Figure 4b), which revealed reduced expression of FOXC2 and FOXC2 promoter activities by the phosphatidylinositol 3-kinase/Akt inhibitor, LY294002, but not by the MEK inhibitor, U0126 (Figure 4b). Treatment with Akt-specific inhibitor and genetically

inhibited Akt activity or expression by expressing dominant-negative Akt expression vector or specific Akt siRNA resulted in suppression of phospho-Akt, FOXC2 and cell mobility in A549 cells (Supplementary Figure S1F). The observation was confirmed by transfecting constitutively activated Akt, myr-Akt, into A549 and H460 cells with or without resveratrol treatment to test the role of Akt in regulating FOXC2 expression. Activation of NF- κ B by Akt has been reported that have the critical role in cell proliferation and EMT.²⁹ The results revealed that constitutively activating Akt rescued the resveratrol-mediated inhibition of NF- κ B activity (Figure 4c), FOXC2 expression, E-cadherin suppression (Figure 4d and Supplementary Figure S1E) and subsequent cell mobility (Figure 4e). These data suggest that Akt signaling, rather than the MAPK signaling pathway, is involved in resveratrol-mediated regulating FOXC2 expression and the MET in lung cancer cells.

The ability of PP2A/C, a catalytic subunit of serine/threonine phosphatase PP2A, to downregulate Akt activity by

Table 1. Clinicopathological characteristics of lung cancer patients with associated FOXC2 expression

Characteristics	FOXC2 low (n = 48)	FOXC2 high (n = 48)	P-value
Gender			
Female	23	28	0.3055
Male	25	20	
Stage, no. of patients			
I-II	22	19	0.5376
III-IV	26	29	
Tumor status, no. of patients			
T1	39	34	0.2318
T2-T4	9	14	
Node status, no. of patients			
N0	23	10	*0.0052
N1-N3	25	38	
Distant metastasis, no. of patients			
M0	33	32	0.8231
M1	15	16	

* $P < 0.05$. Significances of association were determined using a χ^2 test.

dephosphorylating Akt has been reported.³⁰ The involvement of PP2A/C in the resveratrol-mediated signaling cascade and biological functions was examined in lung cancer cells. Treatment with resveratrol increased the expression and activity of PP2A/C protein in a dose- and time-dependent manner (Figures 5a,b). The role of PP2A/C in resveratrol-mediated regulation of the signaling cascade, FOXC2 expression, and cell migration/invasion was determined by treating A549 cells with resveratrol in the presence of okadaic acid, a PP2A/C inhibitor. This treatment resulted in decreased PP2A/C expression and abolished the inhibitory effects of resveratrol on Akt activation and FOXC2 expression (Figure 5c). Genetically knocking down PP2A/C by expressing specific PP2A/C siRNA (siPP2A/C) in A549 cells recovered resveratrol-inhibited Akt phosphorylation, FOXC2 expression and cell mobility (Figures 5d–e). The siPP2A/C rescued resveratrol-suppressed NF- κ B activity in the F6 reporter, but not in the F6/mutNF- κ B reporter (Figure 5d). These findings indicated that resveratrol inhibits FOXC2 expression and cell mobility by regulating the PP2A/C –| Akt \rightarrow NF- κ B signaling cascade.

We next investigated the prognostic significance of PP2A/C and the correlation of PP2A/C expression with FOXC2 levels in human lung cancer patients based on PP2A/C scores (Supplementary Figure S3) and the relationships between PP2A/C expression levels and lung cancer clinicopathological characteristics (Table 2). High-PP2A/C expression levels (scores of 2 and 3) correlated with better prognosis, better overall survival, and longer disease-free interval than tumors with low PP2A/C expression levels (scores of 0 and 1) (Figure 5f). Lung cancer specimens analyzed by immunohistochemistry had an inverse correlation between expression of FOXC2 and PP2A/C as tested by Spearman's nonparametric correlation test (correlation coefficient = -0.174 , $P < 0.05$) (Supplementary Table S1). Representative immunohistochemical staining for PP2A/C and FOXC2 on serial sections revealed inverse staining patterns in lung cancer tissues (Supplementary Figure S4A). The correlation of high-FOXC2 expression with low-PP2A/C expression in human lung cancer patients is consistent with our finding that knockdown of PP2A/C upregulates FOXC2 expression in lung cancer cells (Figure 5d).

miR-520h has a crucial role in resveratrol-mediated PP2A/C induction and FOXC2 expression

miRNA has been documented as a key regulator in cancer progression.³¹ According to our previous study,³² PP2A/C could be

regulated by the expression of miR-520h and contribute to anticancer activity. Therefore, we speculated that miR-520h may involve in the resveratrol-mediated regulation of PP2A/C. In the presence of resveratrol, expression of miR-520h was significantly suppressed in a dose-dependent manner (Figure 6a). We also found that expression of miR-520h decreases the protein expression of PP2A/C in a dose-dependent manner (Supplementary Figure S4B). In addition, the resveratrol-mediated PP2A/C induction was abolished after restoring the expression of miR-520h, followed by rescued FOXC2 expression (Figure 6b). These results suggest a crucial role of resveratrol in the regulation of miR-520h, which functions on regulating PP2A/C expression and subsequent FOXC2 inhibition. The functional role of miR-520h was investigated by determining the migration and invasion abilities of resveratrol-treated lung cancer cells. In contrast to the inhibition of migration/invasion in control vector expressed A549 (A549/Ctrl) cells, overexpression of miR-520h mitigated the resveratrol-suppressed cell migration/invasion (Figure 6c, lane 1, 2 and 4, 5). Moreover, expression of a PP2A/C construct lacking 3'UTR significantly inhibited migration/invasion ability both in A549/Ctrl and A549/miR-520h cells (Figure 6c, lane 1, 3 and 4, 6). To further assess the contribution of miR-520h to FOXC2 expression and cell mobility, we performed *in vitro* loss-of-function analyses by silencing the endogenous miR-520h using a modified antisense miR-520h inhibitor (antagomiR-520h, Ambion, Austin, TX, USA). Administration of antagomiR-520h decreased the endogenous level of miR-520h as detected by quantitative reverse transcriptase–polymerase chain reaction (qRT–PCR) (Supplementary Figure S5A) in A549 and other lung cancer cell lines. Treatment with antagomiR-520h increased the expression of PP2A/C and E-cadherin, but reduced the expression of FOXC2 and Vimentin (Supplementary Figure S5A). At 48 h after transfection of the miR-520h inhibitor, but not a control miRNA inhibitor, the capacity of lung cancer cells to migrate and invade was significantly reduced (Supplementary Figure S5B). These evidences suggest the functional role of miR-520h in resveratrol-mediated PP2A/C inhibition and reduced cell invasion.

To further ascertain whether expression of miR-520h correlated with the poor clinicopathological characteristics of lung cancers, we used qRT–PCR to analyze miR-520h expression in 106 human lung cancer specimens. The relationship between the level of miR-520h expression and the clinicopathological characteristics of the lung tumors is summarized in Table 3, in which patients whose tumors expressed high levels of miR-520h demonstrated more advanced tumor stages, status and lymph node metastases compared with patients whose tumors expressed low levels of miR-520h. Next, we examined the role of miR-520h in a cohort of the patients with lung cancer that had long-term follow-up. Using qRT–PCR, miR-520h expression was assayed among the tumors and separated into high expression and low expression. Both Log-rank analysis (Figure 6d) and univariate Cox model including miR-520h level and tumor node metastasis (TNM) status (Supplementary Table S2) indicated that disease-free and overall survivals were significantly worse in patients with higher ($n = 53$) miR-520h expression in their tumor tissues compared with the patients with low miR-520h ($n = 53$) expression (Figure 6d). This became evident that high-miR-520h expression was accompanied by a worse clinical outcome.

DISCUSSION

The therapeutic potential and the action mechanisms of naturally occurring phytochemicals have been of great interest throughout history. Resveratrol, a lead compound in clinical trials, induces arrest of growth and mitigates inflammation by regulating apoptotic and inflammatory signaling pathways such as p53 and prostaglandin production in human cancers.³³ Numerous *in vivo* and clinical studies have documented its chemopreventive effects and its antitumor effects that prevent cancer progression,

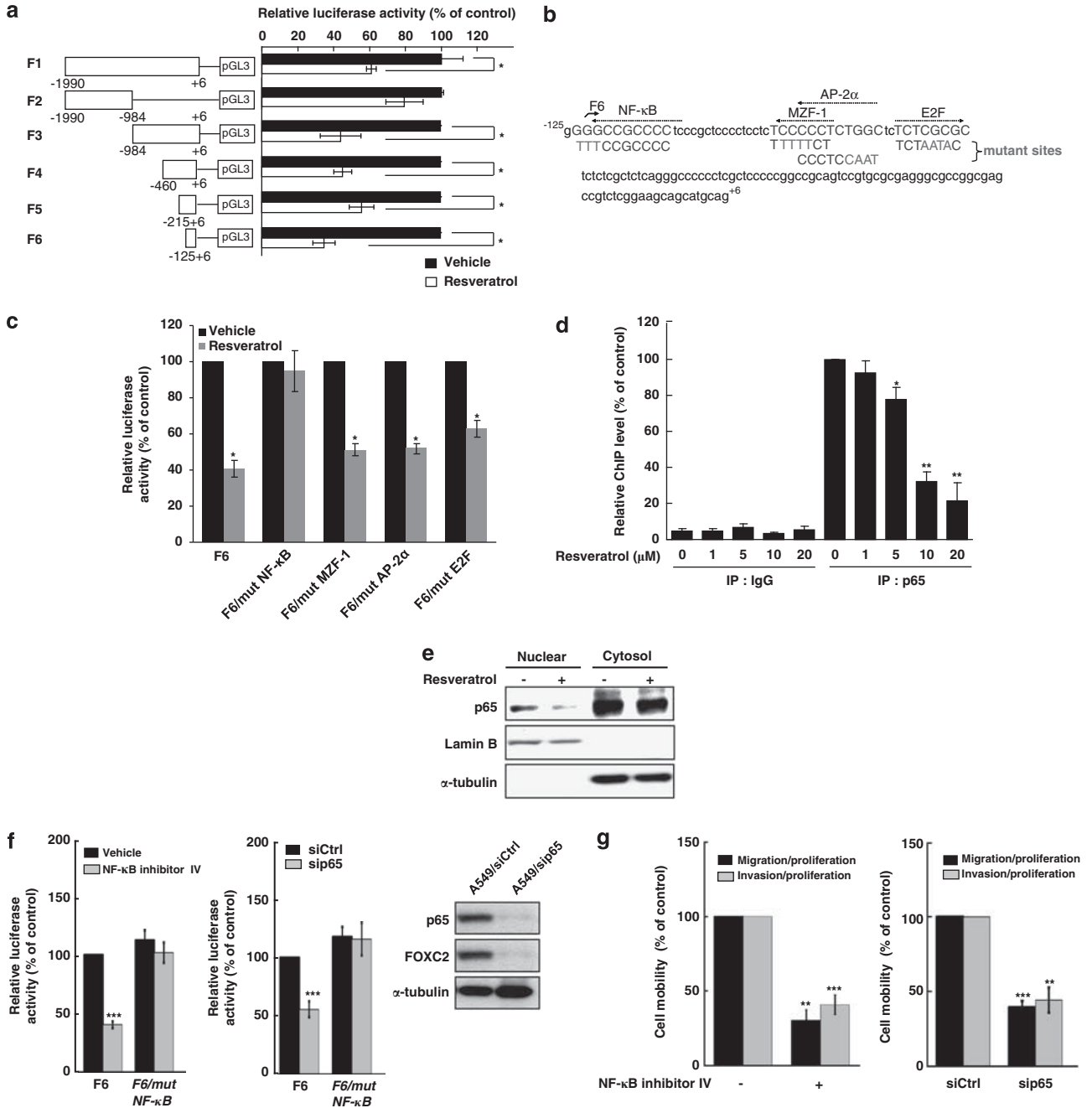


Figure 3. Resveratrol affected *FOXC2* promoter activity. **(a)** Luciferase reporter assays used a series of 5' promoter deletion mutants of the *FOXC2* gene (F1–F6). The ~1.9-kb fragment upstream of the start codon contains the transcription factor-binding elements. The CL1-5 cells were transfected with the reporter constructs in the presence or absence of 20 μM resveratrol and luciferase activity was measured 48 h after transfection. Bars represent means \pm s.d. from three independent experiments in triplicates and asterisks denote a significant difference compared with values for untreated control (* indicates $P < 0.05$). **(b)** Schematic representation of the ~130-bp region of human *FOXC2* promoter (–125 to +6) where arrows indicate potential binding sites for AP-2 α , NF- κ B, MZF-1 and E2F, each mutant binding site is shown, and mutated residues are exhibited in red. **(c)** Activity of *FOXC2* promoter with different mutant binding sites measured based on luciferase activity 48 h after transfection. Bars represent means \pm s.d. from three independent experiments in triplicate and asterisks denote a significant difference compared with values for untreated control. (* indicates $P < 0.05$). **(d)** The binding of the p65 and *FOXC2* promoter was analyzed by chromatin immunoprecipitation assay (ChIP) with a p65 antibody in A549 cells with or without resveratrol treatment. Data are representative of at least three independent experiments performed in triplicate. **(e)** Nuclear translocation of p65 was measured after resveratrol treatment using lamin B as a nuclear marker and α -tubulin as a cytosolic marker. **(f)** The role of NF- κ B in the reporter activities of the F6 *FOXC2* and F6/mut NF- κ B *FOXC2* reporter were measured by luciferase reporter assay. All experiments were performed in at least three separate experiments. The expression of p65 and *FOXC2* was analyzed by western blot assay. **(g)** The functional role of NF- κ B on the transwell migration assay and Matrigel invasion assay was examined in A549 cells treatment with NF- κ B inhibitor IV or expressing siControl (siCtrl) or sip65. Bars indicate mean \pm s.d., and asterisks denote a significant difference. Data are representative of at least three independent experiments performed in triplicate. A full colour version of this figure is available at the *Oncogene* journal online.

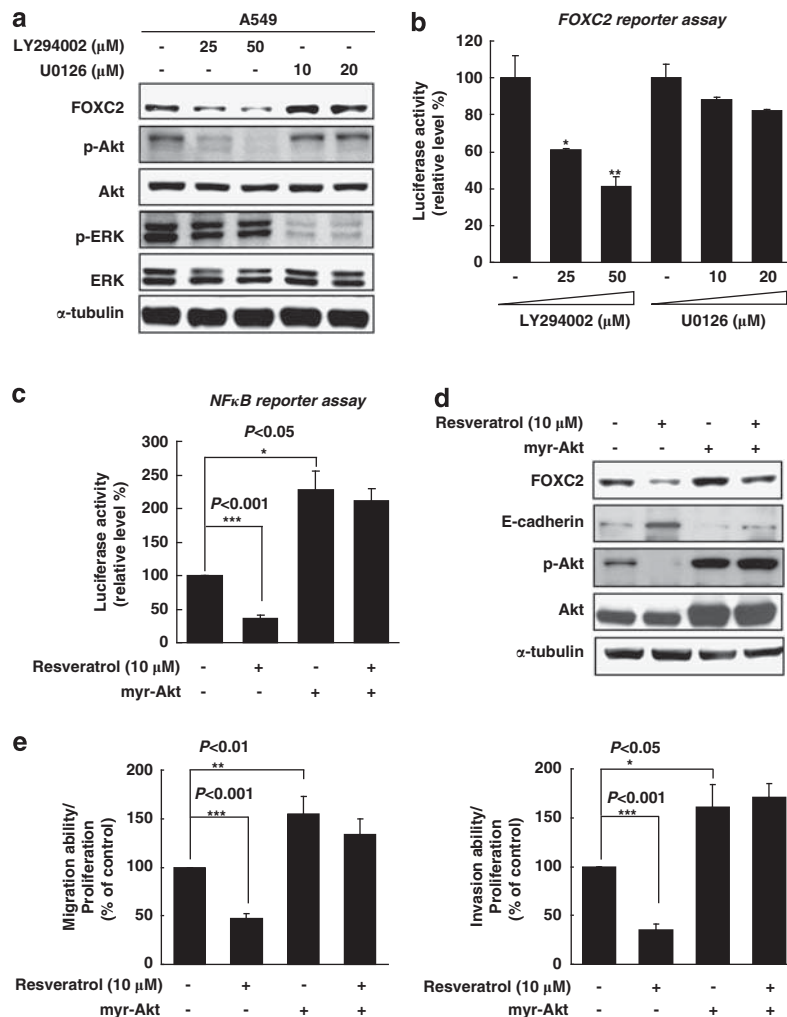


Figure 4. Akt affects resveratrol-suppressed FOXC2 expression and cell mobility through NF-κB regulation. **(a)** The effects of phosphatidylinositol 3-kinase (PI3K)/Akt inhibitor (LY294002) and MAPK inhibitor (U0126) on FOXC2 expression were studied by collecting lysates from A549 cells treated with the indicated concentrations of the chemical inhibitors. **(b)** The promoter activity of FOXC2 was affected by the PI3K/Akt inhibitors. The FOXC2 reporter assay used the full-length (F1) construct in A549 cells. Bars indicate means ± s.d. and asterisks denote a significant difference compared with values of the untreated control (* indicates $P < 0.05$, ** indicates $P < 0.01$). Data are representative of at least three independent experiments performed in triplicate. **(c)** The role of Akt in resveratrol-mediated NF-κB inhibition was studied by co-transfecting cells with the NF-κB-promoter reporter construct and myr-Akt construct for 48 h, and then treating the cells with resveratrol to assay luciferase activity. Bars indicate mean ± s.d. and asterisks denote a significant difference. Data are representative of at least three independent experiments performed in triplicate. **(d)** The function of Akt in the resveratrol-mediated regulation of FOXC2, E-cadherin, N-cadherin and p-Akt was analyzed by immunoblotting in A549 cells transfected with or without myr-Akt. **(e)** The migration (left) and invasion (right) abilities of resveratrol-treated cells were affected by Akt. Bars represent mean ± s.d. and asterisks denote a significant difference (* indicates $P < 0.05$; **, $P < 0.01$ and ***, $P < 0.001$). Data are representative of at least three independent experiments performed in triplicate.

angiogenesis and metastasis.³⁴ Resveratrol also potentiates the apoptotic effects mediated by cytokines and chemotherapeutic agents.³⁴ This study identifies a novel mechanism of resveratrol that induces MET and suppresses tumor metastasis through the underlying pathway of upregulating miR-520h-mediated PP2A/C expression that consequently inactivates AKT/NF-κB and further inhibits the expression of FOXC2. This study provides evidence of resveratrol treatment functionally regulating MET.

During the progression of cancer, EMT consequently enhances the invasiveness and metastasis ability of cancer cell. Here we have studied the ability of resveratrol to induce MET in cancer cells, which occurs by inhibiting FOXC2 expression. FOXC2 is a crucial transcriptional factor that controls EMT, regulates embryonic development and induces tumor angiogenesis and metastasis.³⁵⁻³⁷ Elevated FOXC2 has been identified in patients with

advanced stages of cancer and poor survival probability.^{13,15} These prior studies and our results indicating the ability of resveratrol to inhibit FOXC2 expression provide evidence of a novel resveratrol function in MET induction. Recent studies have indicated that inducing EMT may result in the formation of cancer stem cells and the induction of anticancer drug resistance.³⁸ As the resveratrol-suppressed expression of FOXC2 dramatically induces MET, resveratrol may also suppress both the maintenance of cancer stem cells and the induction of drug resistance.

Both AKT and MAPKs have been identified as EMT gatekeepers that regulate such key transition factors as SNAIL, SLUG, TWIST and FOXC2.³⁹ Similar to our findings on the role of AKT/NF-κB in regulating FOXC2 expression in lung cancer, expressing FOXC2 is known to be regulated by activating AKT and ERK1/2 in endothelial cells and adipocytes.^{27,28} However, as numerous

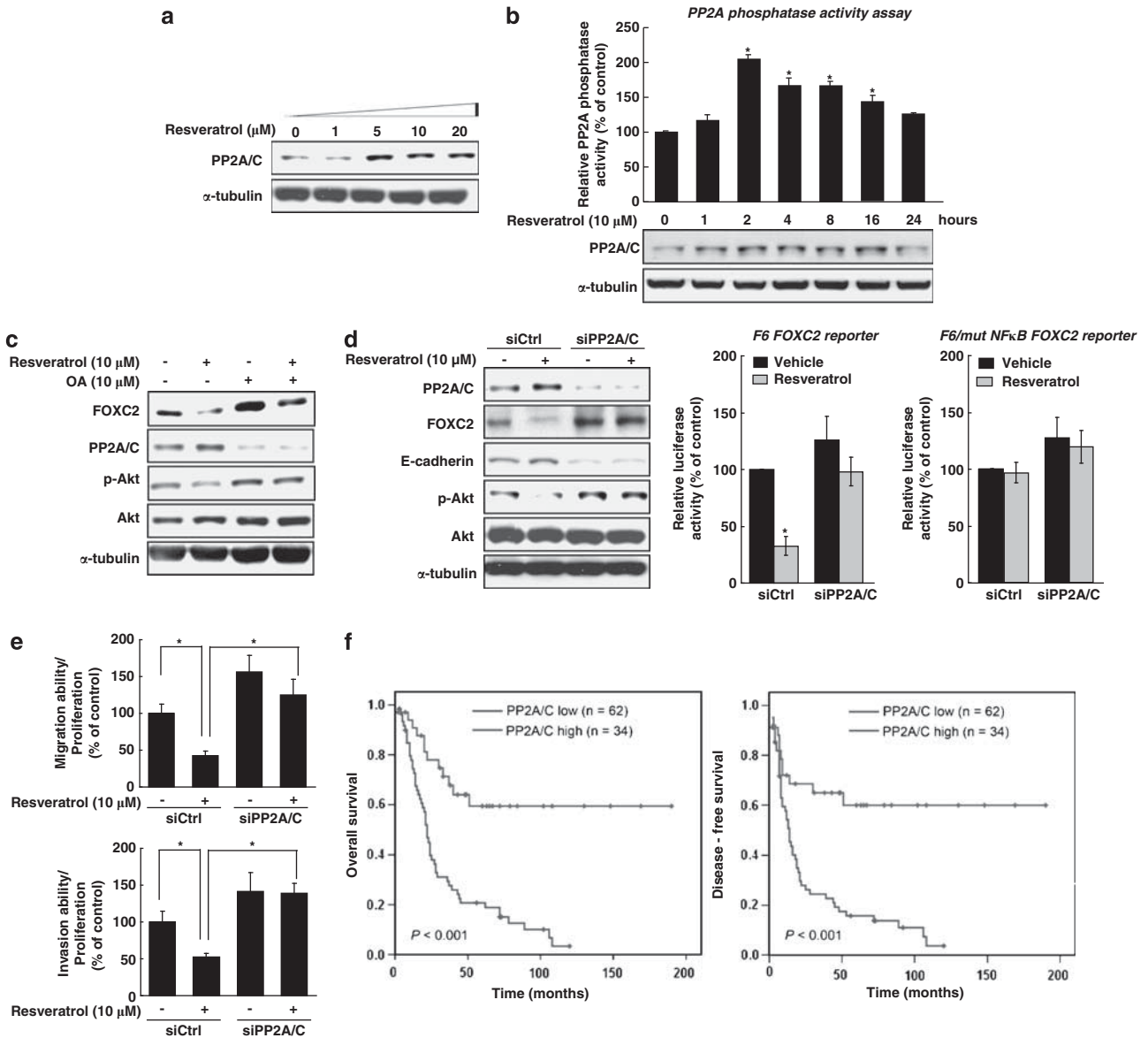


Figure 5. Regulation of the resveratrol-induced signaling pathway depends on PP2A/C. **(a)** The expression of PP2A/C was induced in A549 cells treated with resveratrol. **(b)** Time-dependent changes in PP2A phosphatase activity and expression in A549 cells treated with resveratrol. Bars indicate mean \pm s.d. and asterisks denote a significant difference compared with values for untreated control (* indicates $P < 0.05$). Data are representative of at least three independent experiments performed in triplicate. **(c)** The PP2A inhibitor OA affected Akt activation and FOXC2 expression. Cells pretreated with vehicle or 10 μ M of OA for 4 h and then treated with resveratrol to analyze the expression of PP2A/C, FOXC2 and phosphorylated Akt. **(d)** The role of PP2A/C in resveratrol-induced signaling cascades was examined by knocking down PP2A/C in A549 cells with siPP2A/C and analyzing the expression of PP2A/C, FOXC2, E-cadherin and phosphorylated Akt in cell lysates (left) and the reporter activities of the F6 FOXC2 and F6/mut NF- κ B FOXC2 reporter (right). All experiments were performed in at least three separate experiments. **(e)** The functional role of PP2A/C on the transwell migration assay (top) and Matrigel invasion assay (bottom) was examined in A549 cells expressing siControl (siCtrl) or siPP2A/C. Bars indicate mean \pm s.d. and asterisks denote a significant difference. Data are representative of at least three independent experiments performed in triplicate. **(f)** The PP2A/C expression level, as determined by IHC staining predicts better clinical outcomes in 96 lung cancer patients when differences between the groups were compared with the two-sided log-rank test. The Kaplan-Meier curves analyze overall (left) and disease-free (right) survival in lung cancer patients.

studies have indicated that AKT and NF- κ B are frequently activated in human cancers and have critical roles in drug resistance and metastasis, we speculate that resveratrol may also function through other AKT/NF- κ B-dependent mechanisms to suppress cancer progression, in addition to inhibiting FOXC2. We identify AKT-mediated NF- κ B activation as the pathway leading to EMT that is resveratrol-suppressed and FOXC2-dependent. When Akt activates the NF- κ B pathway, matrix metalloproteinase production is stimulated through the phosphorylation of the I κ B

kinase, resulting in I κ B degradation and further activation of NF- κ B nuclear translocation.^{40,41} Activating NF- κ B by Akt upregulates Snail expression and induces the EMT.⁴² Here, we show that resveratrol downregulating FOXC2 and consequently inducing MET depends on inactivated AKT-mediated NF- κ B. This mechanistic network linking AKT, NF- κ B, FOXC2 and EMT is a potential target for anti-metastatic therapeutics.

A major serine-threonine phosphatase in cells, PP2A, mitigates the aberrant activities of oncogenic kinases expressed in cancer

Table 2. Clinicopathological characteristics of lung cancer patients with associated PP2A/C expression

Characteristics	PP2A/C low (n = 62)	PP2A/C high (n = 34)	P-value
Gender			
Female	38	21	1
Male	24	13	
Stage, no. of patients			
I-II	20	21	*0.0052
III-IV	42	13	
Tumor status, no. of patients			
T1	47	26	0.9203
T2-T4	15	8	
Node status, no. of patients			
N0	16	19	*0.0034
N1-N3	46	15	
Distant metastasis, no. of patients			
M0	37	22	0.6315
M1	25	12	

* $P < 0.05$. Significances of association were determined using a χ^2 test.

cells,⁴³ and has been suggested to regulate the phosphatidylinositol 3-kinase, NF- κ B, MAPK, Wnt and PKC pathways.⁴³ Inactivating PP2A genetically or functionally has been found in human breast, colon, lung tumors and melanoma.⁴⁴ This evidence has identified PP2A as a potential target for tumor suppressor drugs. Activation of PP2A enhanced by forskolin, FTY720 and 1,9-dideoxy-forskolin is currently known to dramatically suppress the development of drug resistance and progression of cancer.⁴⁴⁻⁴⁷ The highly promising role of PP2A in cancer treatment means that discovering new molecules targeting PP2A has become a novel strategy for therapy. Here, we identify the function of resveratrol in activating PP2A, which provide new evidence supporting the therapeutic potential of resveratrol, and precisely explaining the pathway leading to AKT/NF- κ B inactivation.

The newly identified small noncoding RNAs, miRNAs, belong to a novel class of gene regulators that control gene expression by binding to complementary sequences in the 3'UTRs of target mRNAs. Deregulated expression of miRNAs has been reported in human cancers⁴⁸ and may affect multiple steps during metastasis. An example is the miR-200 family of miRNAs, which targets the transcription repressors ZEB1 and ZEB2 to have an emerging role in promoting EMT and metastasis.⁴⁹ The oncogenic- and tumor-suppressive roles of miRNAs have been revealed by several studies, but their function and regulation are still incomplete.³¹ The ability of resveratrol to regulate the miRNA expression of miR-663 and miR-155 has only been investigated in SW480 and THP-1 cells.^{50,51} Here, we provide evidence that resveratrol treatment could inhibit the expression of oncogenic miR-520h. Similar results from a study of the closely-related miR-520c (both belong to the miR-515 gene family) revealed a prometastasis function that induced invasion of MCF-7 cells.⁵² Our study provides a miRNA-mediated sequential pathway triggered by resveratrol: resveratrol \rightarrow miR-520h \rightarrow PP2A/C \rightarrow AKT \rightarrow NF- κ B \rightarrow FOXC2 \rightarrow EMT (Figure 6e). These results shed light on the mechanism of the antitumor effects of resveratrol.

MATERIALS AND METHODS

Reagents and antibodies

Trans-resveratrol, LY294002 (2-4-morpholino)-8-phenyl-4H-1-benzopyran-4-one), and okadaic acid²³ were purchased from Sigma-Aldrich (St Louis,

MO, USA). UO126 (1,4-diamino-2,3-dicyano-1,4-bis(2-aminophenylthio)butadiene) was purchased from Calbiochem (Nottingham, UK). Antibodies to the following were used: E-cadherin (Cell Signaling Technology Inc., Danvers, MA, USA), Fibronectin (BD Biosciences, San Jose, CA, USA), N-cadherin (BD Biosciences), Vimentin (Neomarker, Fremont, CA, USA), FOXC2 (Abcam, Cambridge, MA, USA), PP2A/C (Cell Signaling Technology Inc.), Akt (Cell Signaling Technology Inc.), anti-phospho-extracellular signal-regulated kinase 1/2 (Cell Signaling Technology Inc.), anti-phospho-Akt (Thr308, Cell Signaling Technology Inc.), NF- κ B (Cell Signaling Technology Inc.), Twist (Santa Cruz Technology, Santa Cruz, CA, USA), Slug (Santa Cruz Technology), Snail (Santa Cruz Technology), E2F (Santa Cruz Technology), MZF-1 (Santa Cruz Technology), AP2 α (Santa Cruz Technology), IgG (Santa Cruz Technology) and α -tubulin (Sigma-Aldrich).

Cell culture

The GP + E86 and PA317 cell lines were cultured in Dulbecco's Modified Eagle Medium (GIBCO, Invitrogen, Carlsbad, CA, USA). The lung cancer cell lines, CL1-5, A549, H322 and H1435 cell lines, and HEK293T human embryonic kidney fibroblast cells, were maintained in Dulbecco's Modified Eagle Medium/F12 (1:1) (Hyclone Laboratories, Logan, Utah, USA). NCI-H520 cells were cultured in RPMI-1640 (Hyclone Laboratories). The A549/siPP2A/C and CL1-5/siPP2A/C cells were cultured in Dulbecco's Modified Eagle Medium/F12 medium containing puromycin 2 μ g/ml (Sigma-Aldrich). Medium were supplemented with 10% fetal bovine serum and antibiotics (100 unit/ml penicillin G and 100 μ g/ml streptomycin). Cells were incubated at 37 $^{\circ}$ C in a humidified 5% CO₂ atmosphere.

Establish stable cell line by retrovirus infection

The human FOXC2 cDNA was subcloned into the pBabe-Puro vector (Addgene, Cambridge, MA, USA). A retroviral vector expressing either the FOXC2 gene or the control vector was transfected into an ecotropic packaging cell line, GP + E86, by lipofectamin LTX (Invitrogen), incubated overnight, and harvested. A total of 8 μ g/ml polybrene was added to the supernatants in 3 ml medium for the cells of the second packing cell line PA317. After 2 h the complete medium was added to the PA317 cells, and they were incubated overnight and then harvested. Packaging cells were then selected with 2 μ g/ml puromycin. To collect the amphotropic virus from the medium of the PA317 cells so that lung cancer cells could be infected, cells were selected by adding 2 μ g/ml puromycin and then were diluted 1000-fold to obtain single clones.

Western blotting analysis

Cells were lysed in NETN lysis buffer (150 mM NaCl, 20 mM Tris-HCl pH8.0, 0.5% NP40 and 1 mM EDTA) containing a protease inhibitor cocktail (Sigma-Aldrich). Equal amounts of proteins were separated by SDS-PAGE and transferred to PVDF membrane (Millipore Corporation, Billerica, MA, USA). After blocking, the blots were probed with the indicated primary antibodies. After washing and incubating with secondary antibodies, the blots were visualized by ECL reagent (Millipore).

Transwell migration and invasion assays

Migration and invasion assays were performed as described previously.³² Briefly, transwell migration assays used 1×10^5 cells plated in a noncoated top chamber (24-well insert; pore size, 8 μ m; Corning Costar Corning Incorporated, NY, USA) and incubated for 24 h. The invasion assay used 1×10^5 cells plated in a Matrigel-coated top chamber and incubated for 48 h. Each well was coated freshly with 60 μ g Matrigel (BD Bioscience) before the invasion assay. In both assays, cells were plated in medium without serum or growth factors, and medium supplemented with serum was used as a chemoattractant in the lower chamber. The cells were incubated for 24 (migration assay) or 48 h (invasion assay) and cells that did not migrate or invade through the pores were removed by a cotton swab. Cells on the lower surface of the membrane were fixed with methanol and stained with crystal violet. The number of cells migrating through or invading through the

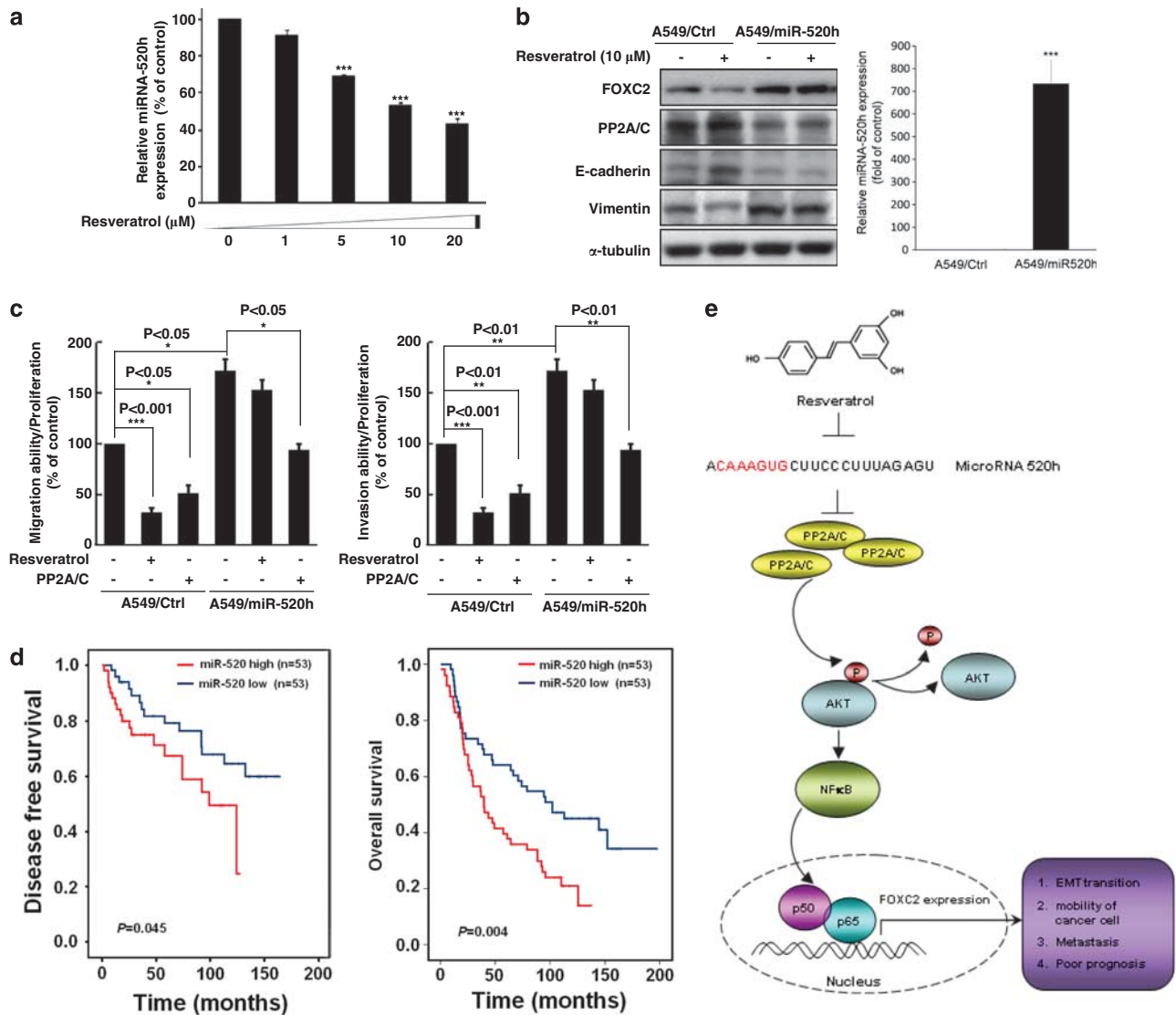


Figure 6. The miR-520h is involved in resveratrol-mediated PP2A expression and subsequent signaling pathway. **(a)** Resveratrol-treated A549 cells had dose-dependent downregulation of miR-520h, as determined by qRT-PCR. Data are representative of at least three independent experiments performed in triplicate. **(b)** Left panel, the role of miR-520h in PP2A/C regulation was determined by collecting cell lysates from control A549 cells (A549/Ctrl) and from A549 cells overexpressing miR-520h (A549/miR-520h) that had both been cultured with or without resveratrol. Right panel, after miRNA transfection, RNA was isolated from A549-transfected cells and the expression of miRNAs was confirmed by qRT-PCR. The data were normalized to the level of U47 RNA in each sample. Asterisks denote a significant difference. Data are representative of at least three independent experiments performed in triplicate. **(c)** The functions of miR-520h in regulating PP2A/C-mediated cell migration and invasion were assayed by comparing A549/Ctrl and A549/miR-520h cells that did or did not receive resveratrol treatment. The expression of PP2A/C was rescued by introducing an expression construct of PP2A/C into both the A549/Ctrl and A549/miR-520h cells. Bars represent mean \pm s.d. and asterisks denote a significant difference (* indicates $P < 0.05$; **, $P < 0.01$ and ***, $P < 0.001$). Data are representative of at least three independent experiments. **(d)** MiR-520h level predicts poor clinical outcome in 106 patients with lung cancer. The log-rank test (two-sided) was used to compare differences between groups. The Kaplan–Meier curves show analyses of disease-free (left) and overall (right) survival in patients with lung cancer. **(e)** A working model shows the molecular mechanism underlying the ability of resveratrol to suppress EMT as human lung cancer progresses.

membrane was counted under a light microscope ($\times 40$, three random fields per well).

Cell tracing by time-lapse microscope image system

Cells were seeded in cell culture dishes and grown in Dulbecco's Modified Eagle Medium/F12 supplemented with 10% fetal bovine serum. After 7 h, cells were set down on a fluorescence microscope (Axioplan 2, Zeiss, Oberkochen, Germany) equipped with a charge-coupled device camera (Axiocam, Zeiss) and incubated at 37 $^{\circ}\text{C}$ in a humidified 5% CO_2

atmosphere. The cells were imaged every 15 min for a 24-hour period and quantified with the image J system.

Cell viability by MTS (3-(4,5-dimethylthiazol-2-yl)-5-(3-carboxymethoxyphenyl)-2-(4-sulfophenyl)-2H-tetrazolium) test 5×10^4 cells per well were seeded in 96-well plates in medium containing 1% fetal bovine serum. Cells were allowed to adhere for 24 h and were subsequently incubated with the indicated drug concentrations. Each condition was tested in triplicate wells. Viability was assessed by Celltiter96

Table 3. Clinicopathological characteristics of lung cancer patients with associated miR-520 expression

Characteristics	miR-520 low (n = 53)	miR-520 high (n = 53)	P-value
Gender			
Female	22	27	0.3297
Male	31	26	
Stage, no. of patients			
I-II	43	30	*0.0064
III-IV	10	23	
Tumor status, no. of patients			
T1	34	17	*0.001
T2-T4	19	36	
Node status, no. of patients			
N0	37	24	*0.0106
N1-N3	16	29	
Distant metastasis, no. of patients			
M0	50	47	0.2965
M1	3	6	

*P < 0.05. Significances of association were determined using a χ^2 test.

Aqueous1 (Promega, Madison, WI, USA) according to the manufacturer's instructions. The amount of MTT formazan product was analyzed spectrophotometrically at a wavelength of 570 nm. Each individual experiment was repeated at least three times.

Colony formation assay

A total of 5×10^2 cells were seeded in 6-well tissue culture dishes and treated with or without resveratrol. After 7 days, colonies were fixed with 4% paraformaldehyde and stained by 0.05% crystal violet. The total number of colonies in each well was counted.

RT-PCR

Total RNA was isolated using TRIzol (Invitrogen) and reverse transcribed into cDNA using M-MLV reverse transcriptase (Invitrogen). The sequences of the primers were: 5'-GCCTAAGGACCTGGTGAAGC-3' (sense) and 5'-TTGACGAAGCACTCGTTGAG-3' (antisense) for human FOXC2, and 5'-GCTCGTCGTCGACAACGGCTC-3' (sense) and 5'-CAAACATGATCTGGGT CATCTTCTC-3' (antisense) for human β -actin. The reaction mixture was first denatured at 94 °C for 5 min. The PCR conditions for FOXC2 were 94 °C for 30 s, 56 °C for 30 s and 72 °C for 30 s for 35 cycles, whereas for β -actin, they were 94 °C for 30 s, 55 °C for 30 s and 72 °C for 30 s for 22 cycles followed by 72 °C for 10 min.

Specimens and immunohistochemistry

The tissue specimens were obtained from the Cancer Tissue Core of the National Taiwan University Hospital. None of the patients had received preoperative neoadjuvant chemotherapy or radiation therapy. The surgical specimens had been fixed in formalin and embedded in paraffin before being archived. The archived specimens were used for immunohistochemical staining. The histological diagnosis of lung adenocarcinoma was made according to WHO recommendations. The tumor size, local invasion, lymph node metastasis and final disease stage were determined as described previously.⁵³ Follow-up of patients was carried out up to 200 months. Patients who died of postoperative complications within 30 days after surgery were excluded from the survival analysis. A four-point staining intensity scoring system was devised for determining the relative expression of FOXC2 and PP2A/C in cancer specimens; the staining intensity score ranged from 0 (no expression) to 3 (maximal expression). The results were classified into two groups according to the intensity and

extent of staining: the low-expression group had either no staining present (staining intensity score = 0) or positive staining detected in < 10% of the cells (staining intensity score = 1), whereas in the high-expression group had positive immunostaining was present in 10-30% of the cells (staining intensity score = 2) or > 30% (staining intensity score = 3). All immunohistochemical staining results were reviewed and scored independently by two pathologists. Lung cancer tissue sections were deparaffinized, soaked in 10 μ M sodium citrate buffer and boiled in a microwave for 15 min at 500 W to retrieve cell antigens. The primary antibodies, which were mouse monoclonal anti-FOXC2 (1:100; Abnova, Taipei, Taiwan) and rabbit polyclonal anti-PP2A/C (1:25; Cell Signaling), were applied to the slides and incubated at 4 °C overnight. The slides were washed and then the samples were stained by the avidin-biotin-peroxidase method (LSAB + System HRP; Dako, Kyoto, Japan) and counterstained with hematoxylin.

Construct of luciferase reporters

The FOXC2 promoter (nucleotides -1990 to +6) was amplified by PCR (sense: 5'-TGCTCGAGTGCCCAACCAGACCAGCAAC-3' and antisense: 3'-ACTAAGCTTCTGCGTCTGCTCCGAGAC-5') using the BAC clone (RP11-1017A18, Invitrogen) as the template. The PCR product was inserted into the XhoI/HindIII site of the pGEM T-easy vector (Promega). The fragment was subcloned into the pGL3-basic reporter (Promega). Series deletions of FOXC2 promoter reporter constructs were established by using the primer sequences from -984 to +6 of 5'-ACTAAGCTTCTGCGTCTGCGTCCGAGAC-3' (sense) and 3'-ACTAAGCTTCTGCGTCTGCTCCGAGAC-5' (antisense) and by using the primer sequences from -215 to +6 of 5'-TGCTCGAGATCCGCCCGTCCGCTGAAG-3' (sense) and 3'-ACTAAGCTTCTGCGTCTGCTCCGAGAC-5' (antisense). The restriction enzyme BlnI digested the FOXC2-promoter from -984 to +6 to generate a FOXC2-promoter from -460 to +6. Digestion of the FOXC2-promoter from -460 to +6 by the restriction enzyme SmaI generated a FOXC2-promoter from -215 to +6. The mutant luciferase reporters F6/mutE2F (sense: 5'-CCCTCTGGTCTCTAATACTCTCTCGCTCTC-3' and antisense: 5'-GAGAGCGAGAGAGATTAGAGAGCCAGAGGG-3'), F6/mutNF- κ B (sense: 5'-CGCGTCTAGCCCGTTCCGCCCTCCCGC-3' and antisense: 5'-GCGGGAGGGGCGAAACGGGCTAGCAGCG-3'), F6/mutAP-2 α (sense: 5'-CCTCTCTCCCTCCAATTCTCTCGCGCTCTC-3' and antisense: 5'-GAGAGCGGAGAGAAATGGAGGGGGAGAGGAGG-3') and F6/mutMZF-1 (sense: 5'-GCTCCCTCTCTTTTCTCTGCTCTCTCG-3' and antisense: 5'-CGAGAGAGCCAGAGAAAAGAGGAGGGGAGC-3') were generated by the QuickChange XL Site-Directed Mutagenesis Kit (Stratagene, Santa Clara, CA, USA). We searched for potential transcriptional factor-binding sites on the FOXC2-promoter with TESS 2.0/TFSEARCH ver.1.3 software.²⁵

Luciferase reporter assay

Luciferase reporter assays analyzed luciferase activities by the Luciferase Assay System (Promega) as describe previously.²² Firefly luciferase reporter gene construct and pTK-Renilla luciferase construct (for normalization) were cotransfected at 1 μ g each per well. Cell extracts were prepared 48 h after transfection and luciferase activity was measured by the Dual-Luciferase Reporter Assay System (Promega).

PP2A phosphatase activity assay

Cells were treated with resveratrol at the indicated time points and lysed with NETN lysis buffer containing proteinase inhibitors. Equal amounts of protein were used to analyze PP2A phosphatase activity (Millipore). Briefly, 2 μ g anti-PP2A/C-subunit antibody was added to protein lysates and the samples were rotated at 4 °C overnight and then washed. Phospho-peptide was added to the lysate and the mixture was incubated at 30 °C for 10 min. Next, the malachite green detection solution was added to the lysate, it was incubated for 10 min at room temperature and activity was detected at OD₆₅₀.

Construction and production of shRNA clone in lentiviral vector system

The shPP2A clone TRCN000002486, the pLKO.1-shLuc vector that was shRNA against luciferase act as a control, the pCMV-VSV-G plasmid and the

pCMVdeltaR8.91 plasmid were obtained from National RNAi Core Facility at the Genomics Research Center (Academia Sinica, Taipei, Taiwan). Recombinant lentiviruses were produced by HEK293T cells that were cotransfected with the lentivirus expression plasmid, pCMVdeltaR8.91 and pCMV-VSV-G, using Lipofectamine LTX. The viruses were collected from the culture medium 2 days after transfection. Lung cancer cells were infected with lentivirus containing 8 µg/ml polybrene and selected with 2 µg/ml puromycin.

Animal studies

All animal work was performed in accordance with protocols approved by the Institutional Animal Care and Use Committee of China Medical University. Female severe combined immunodeficient mice, age matched and 4–6 weeks old, were used in assays for tumor growth in a subcutaneous xenograft model and lung colonization metastasis in an experimental metastasis model. For experimental metastasis assays, 1×10^6 viable cells were resuspended in 0.1 ml of phosphate-buffered solution and introduced into the circulation via tail-vein injection. Lung metastasis was quantified 8 weeks after injection. The tumor growth assay used 2×10^6 cells suspended in a 1:1 mixture of phosphate-buffered solution and Matrigel, and subcutaneously transplanted into the back of severe combined immunodeficient mice. The xenograft and metastasis models involved daily intraperitoneal administration of either resveratrol at 20 mg/kg or vehicle control to mice. Tumor development was analyzed by measuring tumor length (L) and width (W) and calculating volume (V) through the formula, $V = LW^2/2$. Lung metastatic colonies were counted with a stereoscopic microscope. The luciferase-based, noninvasive bioluminescent imaging and analysis were performed by the Xenogen IVIS-200 system (Xenogen, Alameda, CA, USA).

Chromatin immunoprecipitation assay

The chromatin immunoprecipitation assay was performed with the EZ ChIP kit (Millipore). Cells were fixed with 1% formaldehyde, washed and lysed. The nuclei were released with SDS lysis buffer and sonicated with a MISONIX Sonicator 3000 (Misonix, Farmingdale, NY, USA). The soluble chromatin at 200 ml per immunoprecipitation assay were diluted 10-fold in ChIP dilution buffer and then the lysate was precleared with protein G-agarose beads (Millipore) for 1 h at 4 °C. Antibodies for either nonimmune IgG or target protein were added to the precleared lysate and the mixtures were rotated overnight at 4 °C. The immunocomplexes were pulled down by protein G-agarose beads and then washed with the low-salt wash buffer, the high-salt wash buffer, the LiCl wash buffer and finally two times with Tris-EDTA buffer. The bound protein was eluted with elution buffer containing 1% SDS and 100 mM NaHCO₃. The crosslinks were reversed by overnight incubation at 65 °C. The DNA was purified by the QIAquick PCR purification Kit (QIAGEN, Valencia, CA, USA), and the FOXC2 promoter was amplified by PCR with the 5'-ATCCGCCCGTCCGCTGAAG-3' sense primer and the 5'-CTGCTCGCTCAGGTAGGGCAC-3' antisense primer. Transcripts were detected by quantitative PCR with the LightCycler FastStart DNA Master SYBR Green I kit (Roche Diagnostics, Basel, Switzerland) with the LightCycler 480 (Roche Diagnostics). Cycling conditions were 95 °C for 10 min followed by 35 cycles of 95 °C for 15 s, 55 °C for 10 s and 72 °C for 12 s.

TaqMan miRNA real-time RT-PCR

To determine the expression of miRNA-520h from lung cancer patients, we used TaqMan MicroRNA Assay kit (Applied Biosystems, Carlsbad, CA, USA) following manufacturer's protocol. In all, 10 ng of RNA from patient samples were reverse transcribed using 7 µl of RT mixture containing dNTPs, RT and RNase inhibitor and 3 µl of respective primer. The mixture was incubated at 16 °C for 30 min, 42 °C for 30 min, followed by 85 °C for 5 min. Real-time PCR reactions were then carried out in a total volume of 20 µl reaction mixture containing 1.33 µl of RT product, 10 µl of 2 × Taqman universal PCR master mix, 7.67 µl of water and 1 µl of TagMan assay probe. All reactions, including controls were performed in triplicate. Relative expression of miRNAs was analyzed using Ct method and was normalized by RNU6B expression for patient samples.

Statistical analysis

Results are expressed as mean ± s.d.⁵⁴ as indicated. All statistical tests were two-sided. A value of $P < 0.05$ was considered statistically significant.

CONFLICT OF INTEREST

The authors declare no conflict of interest.

ACKNOWLEDGEMENTS

This work was partially supported by the National Science Council Grant (NSC-2632-B-001-MY3, NSC 96-2320-B-004-MY2, NSC 97-2320-B-039-039-MY3 and NSC 98-2815-C-039-082-B to J-LS); National Health Research Institutes Grant from Taiwan (NHRI-EX98-9712BC, NHRI-EX99-9712BC and NHRI-EX100-9712BC to J-LS); Department of Health, Executive Yuan Grant from Taiwan (DOH99-TD-G111-011 to J-LS); Grants from China Medical University (CMU96-220, CMU97-077 and CMU97-277 to J-LS; CMU-99-NTU-08, CMU100-TS-06 and DMR-101-014 to Y-HY).

Author contributions: J-LS, M-HC, M-CH and M-LK designed and conceived the study. P-SC and J-LS wrote the manuscript. Y-WC, Y-HC, H-AC and Y-JC performed the experiments. C-HW, M-TH, H-AC, Y-HS, W-HH, Y-MJ, C-HH, Y-HJ and MH performed and analyzed the immunohistochemistry experiments.

REFERENCES

- 1 Paget S. The distribution of secondary growths in cancer of the breast. 1889. *Cancer Metastasis Rev* 1989; **8**: 98–101.
- 2 Polyak K, Weinberg RA. Transitions between epithelial and mesenchymal states: acquisition of malignant and stem cell traits. *Nat Rev Cancer* 2009; **9**: 265–273.
- 3 Kim JB, Islam S, Kim YJ, Prudoff RS, Sass KM, Wheelock MJ et al. N-Cadherin extracellular repeat 4 mediates epithelial to mesenchymal transition and increased motility. *J Cell Biol* 2000; **151**: 1193–1206.
- 4 Ngan CY, Yamamoto H, Seshimo I, Tsujino T, Man-i M, Ikeda JI et al. Quantitative evaluation of vimentin expression in tumour stroma of colorectal cancer. *Br J Cancer* 2007; **96**: 986–992.
- 5 Kowalski PJ, Rubin MA, Kleer CG. E-cadherin expression in primary carcinomas of the breast and its distant metastases. *Breast Cancer Res* 2003; **5**: 217–222.
- 6 Zavadil J, Cermak L, Soto-Nieves N, Bottinger EP. Integration of TGF-beta/Smad and Jagged1/Notch signalling in epithelial-to-mesenchymal transition. *EMBO J* 2004; **23**: 1155–1165.
- 7 Timmerman LA, Grego-Bessa J, Raya A, Bertran E, Perez-Pomares JM, Diez J et al. Notch promotes epithelial-mesenchymal transition during cardiac development and oncogenic transformation. *Genes Dev* 2004; **18**: 99–115.
- 8 Barrallo-Gimeno A, Nieto MA. The Snail genes as inducers of cell movement and survival: implications in development and cancer. *Development* 2005; **14**: 3151–3161.
- 9 Alves CC, Carneiro F, Hoefler H, Becker KF. Role of the epithelial-mesenchymal transition regulator Slug in primary human cancers. *Front Biosci* 2009; **14**: 3035–3050.
- 10 Browne G, Sayan AE, Tulchinsky E. ZEB proteins link cell motility with cell cycle control and cell survival in cancer. *Cell Cycle* 2010; **9**: 886–991.
- 11 Hamamori Y, Wu HY, Sartorelli V, Kedes L. The basic domain of myogenic basic helix-loop-helix (bHLH) proteins is the novel target for direct inhibition by another bHLH protein, Twist. *Mol Cell Biol* 1997; **17**: 6563–6573.
- 12 Hartwell KA, Muir B, Reinhardt F, Carpenter AE, Sgroi DC, Weinberg RA. The Spemann organizer gene, Goosecoid, promotes tumor metastasis. *Proc Natl Acad Sci USA* 2006; **103**: 18969–18974.
- 13 Mani SA, Yang J, Brooks M, Schwanning G, Zhou A, Miura N et al. Mesenchyme Forkhead 1 (FOXC2) plays a key role in metastasis and is associated with aggressive basal-like breast cancers. *Proc Natl Acad Sci USA* 2007; **104**: 10069–10074.
- 14 Hader C, Marlier A, Cantley L. Mesenchymal-epithelial transition in epithelial response to injury: the role of Foxc2. *Oncogene* 2010; **29**: 1031–1040.
- 15 Nishida N, Mimori K, Yokobori T, Sudo T, Tanaka F, Shibata K et al. FOXC2 is a Novel Prognostic Factor in Human Esophageal Squamous Cell Carcinoma. *Ann Surg Oncol* 2011; **2**: 535–542.
- 16 Baur JA, Sinclair DA. Therapeutic potential of resveratrol: the *in vivo* evidence. *Nat Rev Drug Discov* 2006; **5**: 493–506.
- 17 Saiko P, Szakmary A, Jaeger W, Szekeres T. Resveratrol and its analogs: defense against cancer, coronary disease and neurodegenerative maladies or just a fad? *Mutat Res* 2008; **658**: 68–94.
- 18 Holmes-McNary M, Baldwin Jr AS. Chemopreventive properties of trans-resveratrol are associated with inhibition of activation of the IκappaB kinase. *Cancer Res* 2000; **60**: 3477–3483.

- 19 Choi HK, Yang JW, Kang KW. Bifunctional effect of resveratrol on the expression of ErbB2 in human breast cancer cell. *Cancer Let* 2006; **242**: 198-206.
- 20 Li Q, Li J, Ren J. UCF-101 mitigates streptozotocin-induced cardiomyocyte dysfunction: role of AMPK. *Am J Physiol Endocrinol Metab* 2009; **4**: 965-973.
- 21 Woo JH, Lim JH, Kim YH, Suh SI, Min DS, Chang JS *et al*. Resveratrol inhibits phorbol myristate acetate-induced matrix metalloproteinase-9 expression by inhibiting JNK and PKC delta signal transduction. *Oncogene* 2004; **23**: 1845-1853.
- 22 Aziz MH, Nihal M, Fu VX, Jarrard DF, Ahmad N. Resveratrol-caused apoptosis of human prostate carcinoma LNCaP cells is mediated via modulation of phosphatidylinositol 3'-kinase/Akt pathway and Bcl-2 family proteins. *Mol Cancer Ther* 2006; **5**: 1335-1341.
- 23 Stewart JR, Ward NE, Ioannides CG, O'Brian CA. Resveratrol preferentially inhibits protein kinase C-catalyzed phosphorylation of a cofactor-independent, arginine-rich protein substrate by a novel mechanism. *Biochemistry* 1999; **38**: 13244-13251.
- 24 Stewart JR, Christman KL, O'Brian CA. Effects of resveratrol on the autophosphorylation of phorbol ester-responsive protein kinases: inhibition of protein kinase D but not protein kinase C isozyme autophosphorylation. *Biochem Pharmacol* 2000; **60**: 1355-1359.
- 25 Heinemeyer T, Wingender E, Reuter I, Hermjakob H, Kel A, Kel O *et al*. Databases on transcriptional regulation: TRANSFAC, TRRD, and COMPEL. *Nucleic Acids Res* 1998; **26**: 364-370.
- 26 Aggarwal BB. Nuclear factor- κ B: The enemy within. *Cancer Cell* 2004; **6**: 203-208.
- 27 Gronning LM, Cederberg A, Miura N, Enerback S, Tasken K. Insulin and TNF alpha induce expression of the forkhead transcription factor gene Foxc2 in 3T3-L1 adipocytes via PI3K and ERK 1/2-dependent pathways. *Mol Endocrinol* 2002; **16**: 873-883.
- 28 Hayashi H, Kume T. Foxc transcription factors directly regulate Dll4 and Hey2 expression by interacting with the VEGF-Notch signaling pathways in endothelial cells. *PLoS One* 2008; **3**: e2401.
- 29 Sun HZ, Yang TW, Zang WJ, Wu SF. Dehydroepiandrosterone-induced proliferation of prostatic epithelial cell is mediated by NF κ B via PI3K/AKT signaling pathway. *Eur J Endocrinol/Eur Fed Endocr Soc* 2010; **204**: 311-318.
- 30 Liao Y HM. A new role of protein phosphatase 2a in adenoviral E1A protein-mediated sensitization to anticancer drug-induced apoptosis in human breast cancer cells. *Cancer Res* 2004; **64**: 5938-5942.
- 31 Garzon R, Marcucci G, Croce CM. Targeting microRNAs in cancer: rationale, strategies and challenges. *Nat Rev Drug Discov* 2010; **9**: 775-789.
- 32 Su JL, Chen PB, Chen YH, Chen SC, Chang YW, Jan YH *et al*. Downregulation of microRNA miR-520h by E1A contributes to anticancer activity. *Cancer Res* 2010; **70**: 5096-5108.
- 33 Athar M, Back JH, Kopelovich L, Bickers DR, Kim AL. Multiple molecular targets of resveratrol: anti-carcinogenic mechanisms. *Arch Biochem Biophys* 2009; **486**: 95-102.
- 34 Aggarwal BB, Bhardwaj A, Aggarwal RS, Seeram NP, Shishodia S, Takada Y. Role of resveratrol in prevention and therapy of cancer: preclinical and clinical studies. *Anticancer Res* 2004; **24**: 2783-2840.
- 35 Kume T, Jiang H, Topczewska JM, Hogan BL. The murine winged helix transcription factors, Foxc1 and Foxc2, are both required for cardiovascular development and somitogenesis. *Genes Dev* 2001; **15**: 2470-2482.
- 36 Sano H, Leboeuf JP, Novitskiy SV, Seo S, Zaja-Milatovic S, Dikov MM *et al*. The Foxc2 transcription factor regulates tumor angiogenesis. *Biochem Biophys Res Commun* 2010; **392**: 201-206.
- 37 Topczewska JM, Topczewski J, Shostak A, Kume T, Solnica-Krezel L, Hogan BL. The winged helix transcription factor Foxc1a is essential for somitogenesis in zebrafish. *Genes Dev* 2001; **15**: 2483-2493.
- 38 Singh A, Settleman J. EMT, cancer stem cells and drug resistance: an emerging axis of evil in the war on cancer. *Oncogene* 2010; **29**: 4741-4751.
- 39 Larue L, Bellacosa A. Epithelial-mesenchymal transition in development and cancer: role of phosphatidylinositol 3' kinase/AKT pathways. *Oncogene* 2005; **24**: 7443-7454.
- 40 Lu Y, Wahl LM. Production of matrix metalloproteinase-9 by activated human monocytes involves a phosphatidylinositol-3 kinase/Akt/IKKalpha/NF-kappaB pathway. *J Leukoc Biol* 2005; **78**: 259-265.
- 41 Agarwal A, Das K, Lerner N, Sathe S, Cicek M, Casey G *et al*. The AKT/I kappa B kinase pathway promotes angiogenic/metastatic gene expression in colorectal cancer by activating nuclear factor-kappa B and beta-catenin. *Oncogene* 2005; **24**: 1021-1031.
- 42 Julien S, Puig I, Caretti E, Bonaventure J, Nelles L, van Roy F *et al*. Activation of NF-kappaB by Akt upregulates Snail expression and induces epithelium mesenchyme transition. *Oncogene* 2007; **26**: 7445-7456.
- 43 Millward TA, Zolnierowicz S, Hemmings BA. Regulation of protein kinase cascades by protein phosphatase 2A. *Trends Biochem Sci* 1999; **24**: 186-191.
- 44 Perotti D, Neviani P. Protein phosphatase 2A (PP2A), a drugable tumor suppressor in Ph1(+) leukemias. *Cancer Metastasis Rev* 2008; **27**: 159-168.
- 45 Neviani P, Santhanam R, Trotta R, Notari M, Blaser BW, Liu S *et al*. The tumor suppressor PP2A is functionally inactivated in blast crisis CML through the inhibitory activity of the BCR/ABL-regulated SET protein. *Cancer Cell* 2005; **8**: 355-368.
- 46 Feschenko MS, Stevenson E, Nairn AC, Sweadner KJ. A novel cAMP-stimulated pathway in protein phosphatase 2A activation. *J Pharmacol Exp Ther* 2002; **302**: 111-118.
- 47 Matsuoka Y, Nagahara Y, Ikeita M, Shinomiya T. A novel immunosuppressive agent FTY720 induced Akt dephosphorylation in leukemia cells. *Br J Pharmacol* 2003; **138**: 1303-1312.
- 48 Esquela-Kerscher A, Slack FJ. Oncomirs - microRNAs with a role in cancer. *Nat Rev Cancer* 2006; **6**: 259-269.
- 49 Korpala M, Kang Y. The emerging role of miR-200 family of microRNAs in epithelial-mesenchymal transition and cancer metastasis. *RNA Biol* 2008; **5**: 115-119.
- 50 Tili E, Michaille JJ, Adair B, Alder H, Limagne E, Taccioli C *et al*. Resveratrol decreases the levels of miR-155 by upregulating miR-663, a microRNA targeting JunB and JunD. *Carcinogenesis* 2010; **31**: 1561-1566.
- 51 Tili E, Michaille JJ, Alder H, Volinia S, Delmas D, Latruffe N *et al*. Resveratrol modulates the levels of microRNAs targeting genes encoding tumor-suppressors and effectors of TGFbeta signaling pathway in SW480 cells. *Biochem Pharmacol* 2010; **80**: 2057-2065.
- 52 Huang Q, Gumireddy K, Schrier M, le Sage C, Nagel R, Nair S *et al*. The microRNAs miR-373 and miR-520c promote tumour invasion and metastasis. *Nat Cell Biol* 2008; **10**: 202-210.
- 53 Chen MW, Hua KT, Kao HJ, Chi CC, Wei LH, Johansson G *et al*. H3K9 histone methyltransferase G9a promotes lung cancer invasion and metastasis by silencing the cell adhesion molecule Ep-CAM. *Cancer Res* 2010; **70**: 7830-7840.
- 54 Kuhn H, Liebers U, Gessner C, Schumacher A, Witt C, Schauer J *et al*. Adenovirus-mediated E2F-1 gene transfer in non-small-cell lung cancer induces cell growth arrest and apoptosis. *Eur Respir J* 2002; **20**: 703-709.

Supplementary Information accompanies the paper on the Oncogene website (<http://www.nature.com/onc>)